and 40.53 MHz, respectively. ^{1}H NMR spectra were recorded on a Varian XL-200 spectrometer. ^{1}H and ^{13}C NMR shifts are reported in ppm downfield of tetramethylsilane. The ^{6}Li chemical shifts are reported in ppm relative to an external 0.3 M ^{6}LiCl/methanol standard. The ^{15}N chemical shifts are reported in ppm relative to an external 0.15 M [^{15}N]aniline/THF standard set at 50 ppm.[9] NMR probe temperatures are accurate to ±2 °C.

The following is a representative procedure for preparing samples for spectroscopic analysis. A stock solution was prepared in a glovebox by sequentially mixing [^{6}Li,^{15}N]$Ph_2NLi_{solvent\text{-}free}$ (20 mg, 0.11 mmol), toluene-d_8 (472 μL), and THF (18 μL, 0.22 mmol). A 5-mm NMR tube was charged sequentially with the pale yellow stock solution (129 μL), toluene-d_8 (840 μL), and THF (31 μL). The tube was placed under septum, removed from the glovebox, and sealed with a flame under reduced pressure.

Colligative Measurements. Solution molalities were measured by freezing-point depression by using a modification of an apparatus described by Seebach[17] interfaced to a Commodore 64 or VIC-20 minicomputer. Samples were prepared in a glovebox and measurements were made under N_2 with standard inert atmosphere techniques. Calibrations were performed with known concentrations of naphthalene in benzene.

[^{15}N]Diphenylamine. Benzenediazocarboxylate (2.9 g, 19.6 mmol) was generated via a literature method.[10] (*Caution: benzenediazocarboxylate is highly explosive when fully dry.*) The diazocarboxylate was suspended in 110 mL of 1,2-dichloroethane and [^{15}N]aniline (950 μL, 10.2 mmol) was added to the suspension. The mixture was heated to 70 °C for 30 min with noted gas evolution. The resultant red-brown solution was concentrated to a brown oil, dissolved in THF, passed through a 2 in. silica gel plug, and evaporated to a red oil. The red oil was multiply flash chromatographed on silica gel (5% ethyl acetate, hexane) to afford [^{15}N]diphenylamine (214 mg, 12.3%) as a white solid. ^{1}H NMR (C_6D_6): δ 7.12 (m, 5 H), 6.86 (m, 5 H), 5.06 (d, J_{N-H} = 88 Hz, 1 H). ^{13}C (^{1}H) NMR (C_6D_6): δ 143.54 (d, J_{N-C} = 14.9 Hz), 129.50, 121.20, 118.13 (d, J_{N-C} = 2.7 Hz).

Solvent-Free Lithium Diphenylamide ($Ph_2NLi_{solvent\text{-}free}$). The various isotopomers of solvent-free lithium diphenylamide were prepared as follows. A 500-mL round-bottom flask fitted to a glass filter frit was charged with diphenylamine (5.27 g, 31.1 mmol) and ethyllithium (1.18 g, 32.8 mmol). To this was added 300 mL of a 2:1 hexane/diethyl ether mixture via vacuum transfer at −78 °C. The milky white solution was warmed to 0 °C and stirred for 1.5 h. The resultant clear solution was concentrated in vacuo to 80 mL and then cooled to −78 °C. Filtration afforded an off-white solid, which was recrystallized from hexane at −78 °C. The resulting white crystalline solid was heated to 80 °C for 24 h under dynamic vacuum to liberate diethyl ether. Sequential washing with 150 mL of near-boiling benzene and 100 mL of near-boiling hexane afforded $Ph_2NLi_{solvent\text{-}free}$ (5.21 g, 95.5%) as an amorphous white solid. ^{1}H NMR (C_6D_6) with 2.0 equiv of 4-picoline: δ 7.95 (picoline) (d, J_{H-H} = 4.69 Hz), 7.56 (d, J_{H-H} = 8.25 Hz), 7.32 (dd, J_{H-H} = 8.19 Hz), 6.80 (dd, J_{H-H} = 8.17 Hz), 6.34 (picoline) (d, J_{H-H} = 5.46 Hz). Anal calcd for $C_{12}H_{10}NLi$: C, 82.29, H, 5.75; Li, 3.96; N, 8.00. Found: C, 82.02; H, 5.67; Li, 3.85; N, 7.82. Detailed ^{6}Li, ^{13}C, and ^{15}N NMR spectroscopic data are found in Tables I and II and Figures 1, 4–6, and 9.

Acknowledgment. We wish to thank the National Science Foundation Instrumentation Program (Grant CHE 7904825 and PCM 8018643) for support of the Cornell Nuclear Magnetic Resonance Facility and the A. P. Sloan Foundation for unrestricted support.

Structure and Reactivity of Lithium Diphenylamide. Role of Aggregates, Mixed Aggregates, Monomers, and Free Ions on the Rates and Selectivities of N-Alkylation and E2 Elimination

Jeffrey S. DePue and David B. Collum*

Contribution from the Department of Chemistry, Baker Laboratory, Cornell University, Ithaca, New York 14853-1301. *Received January 11, 1988*

Abstract: Rate studies of the N-alkylation of lithium diphenylamide with *n*-butyl bromide in THF/hydrocarbon mixtures (THF = tetrahydrofuran) are described. Dramatic induction periods observed for the N-alkylation at low THF concentrations are ascribed to the intervention of reactive mixed dimers of lithium diphenylamide and lithium bromide. In the presence of 1.0 equiv of added lithium bromide, the alkylation rate exhibits a first-order dependence on both the mixed aggregate and *n*-butyl bromide concentrations, supporting a pathway involving direct mixed aggregate alkylation. Incremental changes in the THF concentration uncovered contributions from several additional species. Regions of first or higher order followed by zero-order dependence on the THF concentration are interpreted as an equilibrium shift to a more reactive, highly solvated species assigned as a monomer (or ion pair). At elevated THF concentrations, the alkylation rate increases sharply as a function of the THF concentration, indicating the contribution of an additional, highly solvent dependent alkylation pathway. This latter pathway exhibits fractional-order dependence on the amide concentration, approximate first order dependence on the *n*-butyl bromide concentration, and a seventh-order dependence on the THF concentration. Common ion rate inhibitions by lithium perchlorate and lithium tetraphenylborate, a significant dependence on dielectric effects, and the observed reaction orders implicate a mechanism involving predissociation of free lithium ions. The appearance of competitive eliminations of the *n*-alkyl bromides to form 1-alkenes coincides with the appearance of the free ion alkylation pathway.

Lithium dialkylamides are used routinely throughout organic chemistry as highly reactive and selective bases. Elegant quantitative studies of lithium amides include Streitwieser's[1] and Fraser's[2] ion pair acidity measurements, Newcomb's[3] investigations of amide-mediated hydride transfer, and Huisgen's[4] extensive studies of dehydrohalogenations of aryl halides. However, most

Scheme I

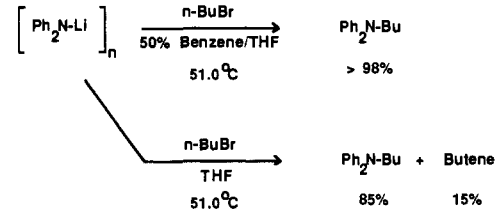

(1) Streitwieser, A., Jr.; Juaristi, E.; Nebenzahl, L. In *Comprehensive Carbanion Chemistry*; Buncel, E., Durst, T., Eds.; Elsevier: New York, 1980; Chapter 7. Gronert, S.; Streitwieser, A., Jr. *J. Am. Chem. Soc.* **1986**, *108*, 7016.

(2) Fraser, R. R.; Mansour, T. S. *J. Org. Chem.* **1984**, *49*, 3442. Fraser, R. R.; Mansour, T. S.; Savard, S. *J. Org. Chem.* **1985**, *50*, 3232. Fraser, R. R.; Mansour, T. S. *Tetrahedron Lett.* **1986**, *27*, 331. Fraser, R. R.; Baignee, A.; Bresse, M.; Hata, K. *Tetrahedron Lett.* **1982**, *23*, 4195. Fraser, R. R.; Bresse, M.; Mansour, T. S. *J. Chem. Soc., Chem. Commun.* **1983**, 620.

(3) Newcomb, M.; Reeder, R. A. *J. Org. Chem.* **1980**, *45*, 1489. Newcomb, M.; Burchill, M. T. *J. Am. Chem. Soc.* **1984**, *106*, 8276. Newcomb, M.; Burchill, M. T. *J. Am. Chem. Soc.* **1984**, *106*, 2450.

(4) Huisgen, R. In *Organometallic Chemistry*; American Chemical Society: Washington, DC, 1960; Monograph Series No. 147, pp 36–87.

0002-7863/88/1510-5524$01.50/0

Scheme II

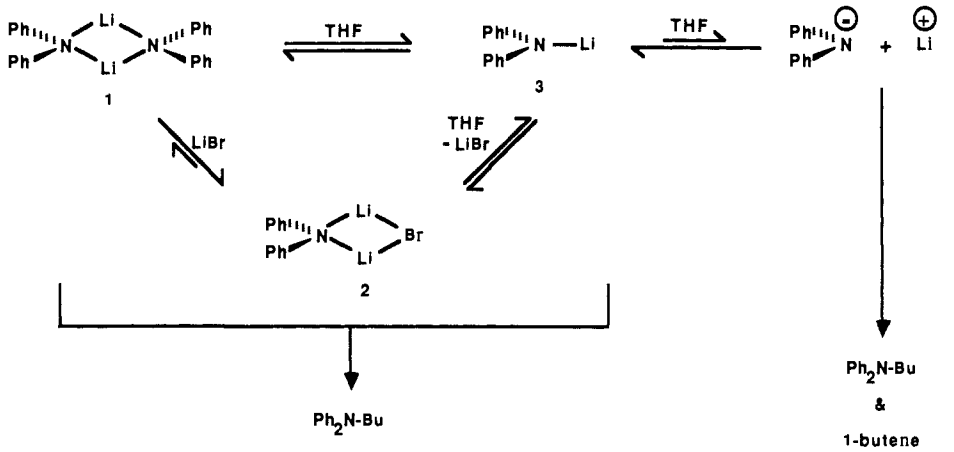

investigations of lithium amides have focused on the events occurring at the electrophiles and have left the detailed dynamics of the amide fragments unexplored.[5,6] Much of the mechanistic insights are based on isotope effects and stereochemistries of eliminations and enolizations. Furthermore, virtually all of the chemistry of lithium amides is founded on very limited knowledge of amide solution aggregation and solvation states.[7-9]

We initiated explorations of lithium amide reactivities and selectivities with the seemingly simple reactions illustrated in Scheme I. Lithium diphenylamide was choosen because of its high thermal stability and the structural similarity to lithiated phenylimines studied previously.[10] The quantitative and irreversible N-alkylation, although clearly not of major synthetic importance,[11] affords a mechanistically transparent system well suited for quantitative rate studies. The competing elimination pathway observed only at high THF concentrations provides a probe of some of the mechanistic principles governing selectivity.[12]

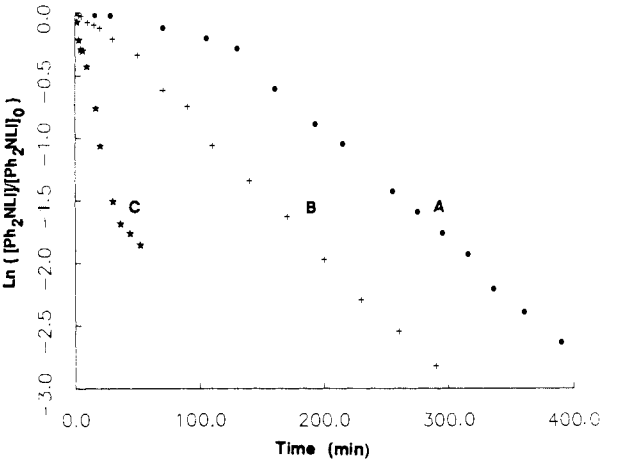

Figure 1. First-order plots of the alkylation of Ph_2NLi (0.015 M) by *n*-BuBr (0.44 M) in the absence of added LiBr at 51.2 °C. (A) 0.44 M THF, (B) 2.23 M THF, and (C) 11.80 M THF.

In the preceding paper we described ^6Li, ^{13}C, and ^{15}N NMR spectroscopic and colligative studies of lithium diphenylamide and its corresponding lithium bromide adduct.[13] In this paper we will describe rate studies of the N-alkylation shown in Scheme I. Conclusions stemming from the mechanistic analysis taken in conjunction with the solution structural studies are summarized in Scheme II. Highlights include (i) the detection of autocatalysis by lithium bromide generated during the course of the alkylation; (ii) the determination of the relative contributions of dimers, mixed dimers, monomers, and free ions to the observed reactivity; (iii) the observation of primary and secondary solvation effects manifested by measured THF reaction orders ranging from zero to seven; (iv) the tracing of the competing elimination product back to only one of the numerous reactive intermediates involved in the alkylation.

Results and Discussion

Throughout the discussions we refer to lithium diphenylamide in the absence of lithium bromide as Ph_2NLi, lithium diphenylamide in the presence of lithium bromide as $Ph_2NLi/LiBr$, and the mixed aggregate with lithium bromide as $Ph_2NLi{\cdot}LiBr$. The latter designation is restricted to discussions of a discrete 1:1 mixed aggregate. Reference to specific aggregation and solvation states include the proper descriptors and graphical representations. References to LiBr in solution do not implicate any specific structural form or solvation state. Numbering is consistent with the previous paper[13] whenever possible.

(5) For leading references, see: d'Angelo, J. *Tetrahedron* **1976**, *32*, 2979. Ireland, R. E., Mueller, R. H., Willard, A. K. *J. Am. Chem. Soc.* **1976**, *98*, 2868. Thummel, R. P.; Rickborn, B. *J. Am. Chem. Soc.* **1970**, *92*, 2064. Miller, D. J.; Saunders, W. H., Jr. *J. Org. Chem.* **1982**, *47*, 5039. McKee, M. L. *J. Am. Chem. Soc.* **1987**, *109*, 559. Moreland, D. W.; Dauben, W. G. *J. Am. Chem. Soc.* **1985**, *107*, 2264. Mass, R. J.; Rickborn, B. *J. Org. Chem.* **1986**, *51*, 1992 and references cited therein.

(6) Pez, G.; Galle, J. E. *Pure Appl. Chem.* **1985**, *57*, 1917. Reimann, W.; Kuivila, H. G.; Farah, D., Apoussidis, T. *Organometallics* **1987**, *6*, 557.

(7) Streitwieser, A., Jr.; Padgett, W. M., II *J. Phys. Chem.* **1964**, *68*, 2916.

(8) Solution structures of N-lithiated species: Reed, D.; Barr, D.; Mulvey, R. E.; Snaith, R. *J. Chem. Soc., Dalton Trans.* **1986**, 557. Armstrong, D. R.; Barr, D.; Clegg, W., Mulvey, R. E., Reed, D., Snaith, R., Wade, K. *J. Chem. Soc., Chem. Commun.* **1986**, 869. Barr, D.; Clegg, W.; Mulvey, R. E.; Snaith, R. *J. Chem. Soc., Chem. Commun.* **1984**, 285. Kimura, B. Y.; Brown, T. L. *J. Organomet. Chem.* **1971**, *26*, 57. Wannagat, U. *Adv. Inorg. Chem. Radiochem.* **1964**, *6*, 225. Wannagat, U. *Pure Appl. Chem.* **1969**, *19*, 329. Jackman, L. M.; Scarmoutzos, L. M.; Porter, W. *J. Am. Chem. Soc.* **1987**, *109*, 6524. Jackman, L. M.; Scarmoutzos, L. M. *J. Am. Chem. Soc.* **1987**, *109*, 5348. Jackman, L. M.; Scarmoutzos, L. M.; Smith, B. D.; Williard, P. G. *J. Am. Chem. Soc.*, in press. Seebach, D.; Bauer, von W. *Helv. Chim. Acta* **1984**, *67*, 1972. Barr, D.; Snaith, R.; Mulvey, R. E.; Wade, K.; Reed, D. *Magn. Reson. Chem.* **1986**, *24*, 713. See also ref 10.

(9) The crystal structure of monomeric lithium diphenylamide chelated by pentamethylethylenediamine (PMDETA) has been reported: Bartlett, R. A.; Dias, H. V. R.; Hope, H.; Murray, B. D.; Olmstead, M. M.; Power, P. P. *J. Am. Chem. Soc.* **1986**, *108*, 6921.

(10) Kallman, N.; Collum, D. B. *J. Am. Chem. Soc.* **1987**, *109*, 7466. Wanat, R. A.; Collum, D. B.; Van Duyne, G.; Clardy, J.; DePue, R. T. *J. Am. Chem. Soc.* **1986**, *108*, 3416.

(11) N-alkylations: Li, X.; Pan, H.; Jiang, X. *Tetrahedron Lett.* **1987**, *28*, 3699. Corriu, R. J. P.; Moreau, J. J. E.; Vernhet, C. *Tetrahedron Lett.* **1987**, *28*, 2963. Uyehara, T.; Asao, N.; Yamamoto, Y. *J. Chem. Soc., Chem. Commun.* **1987**, 1410. Rathke, M. W.; Sullivan, D. *Tetrahedron Lett.* **1986**, *27*, 4249. Herrman, J. L.; Kieczykowksi, G. R.; Schlessinger, R. H. *Tetrahedron Lett.* **1973**, 2433. Huisgen, R.; Mack, W. *Chem. Ber.* **1960**, *93*, 412. Kowalski, C.; Creary, X.; Rollin, A. J.; Burke, M. C. *J. Org. Chem.* **1978**, *43*, 2601. Meyers, A. I. *J. Org. Chem.* **1977**, *42*, 2653. Comins, D. L.; Brown, J. D.; Mantlo, N. B. *Tetrahedron Lett.* **1982**, *23*, 3979. Pez, G. P.; Galle, J. E. *Pure Appl. Chem.* **1985**, *57*, 1917. Petrov, A. A.; Kromer, V. A. *Zh. Obshch. Khim.* **1960**, *30*, 3890. Sanger, A. R. *Inorg. Nucl. Chem. Lett.* **1973**, *9*, 351. Tzschach, A.; Reiss, E. *J. Organomet. Chem.* **1967**, *8*, 255. Liebeskind, L. S.; Welker, M. E.; Fengl, R. W. *J. Am. Chem. Soc.* **1986**, *108*, 6328.

(12) For references to amide-mediated dehydrohalogenations and reviews on eliminations, see: Kopka, I. E.; Nowak, M. A.; Rathke, M. W. *Synth. Commun.* **1986**, *16*, 27.

(13) DePue, J. S.; Collum, D. B. *J. Am. Chem. Soc.*, preceding manuscript in this issue.

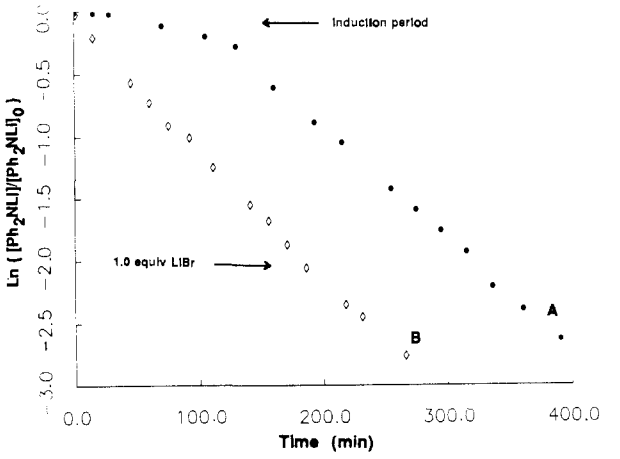

Figure 2. First-order plots of the alkylation of Ph_2NLi (0.015 M) by *n*-BuBr (0.44 M) at 51.2 °C. (A) 0.44 M THF in the absence of added LiBr, (B) 0.44 M THF with 1.0 equiv of added LiBr.

N-Alkylation of Ph_2NLi: Autocatalysis by LiBr. Convenient N-alkylation rates of Ph_2NLi were obtained with *n*-butyl bromide by using 0.015 M Ph_2NLi solutions in benzene/THF at 51.2 ± 0.1 °C. Ph_2NLi exhibits identical reactivities whether it is first isolated as a solvent-free, analytically pure white powder or generated in situ from diphenylamine and purified ethyllithium.[14] The THF and *n*-BuBr were used in large excess (≥30 equiv; ≥0.44 M) so as to maintain pseudo-first-order conditions. Alkylations at low THF concentrations are virtually quantitative as shown by ^1H NMR and gas chromatographic analyses. The disappearance of Ph_2NLi and formation of *n*-butyldiphenylamine were monitored by GC analysis of aliquots quenched by cannulation into 1:1 THF/ethanol.

Representative results are illustrated as first-order plots in Figure 1. At low THF concentration, a dramatic induction period is visible throughout the first reaction half-life (curve A). After completion of the first half-life, the reaction follows well-behaved *first-order* kinetics beyond the fourth half-life. At the intermediate and high THF concentrations (>2.2 M; >18% by volume) the induction periods are not apparent (curves B and C). As the THF concentrations exceed 7.33 M (60%), incomplete conversion to the N-alkylated amine is evidenced by the distinct upward curvature (curve C). In neat THF the reaction cannot be forced beyond 87% conversion. Heating a solution of Ph_2NLi in neat THF to 51 °C for 24 h prior to the addition of the *n*-BuBr shows no effect on the percent conversion, thus ruling out solvent deprotonation[15] as a significant reaction pathway. The incomplete alkylation was traced to a competing elimination producing 1-butene. Additional data and discussion of the elimination pathway are presented later.

The induction periods observed at low THF concentrations were traced to the autocatalytic formation of LiBr. Upon the addition of 1.0 equiv of LiBr to the amide at the onset, the induction period is eliminated and clean first-order behavior is observed to greater than 4 half-lives (Figure 2). The first-order behavior was confirmed when a 10-fold decrease in the Ph_2NLi/LiBr initial concentration showed only an 8% decrease in k_{obsd}. The absence of fractional-order kinetics often coincident with dissociative preequilibria[16] is notable. Addition of 1.0 equivalent of n-butyldiphenylamine shows no measurable effect on the induction period or reaction rate.

(14) Lewis, H. L.; Brown, T. L. *J. Am. Chem.* Soc. **1970**, *92*, 4664.
(15) Eaton, P. E.; Higuchi, H.; Millikan, R. *Tetrahedron Lett.* **1987**, *28*, 1055. Kopka, I. E.; Fataftah, Z. A.; Rathke, M. W. *J. Org. Chem.* **1987**, *52*, 448. De Koning, L. J.; Nibbering, N. M. M. *J. Am. Chem. Soc.* **1987**, *109*, 1715.
(16) Leading references: (a) *Ions and Ion Pairs in Organic Reactions*; Szwarc, M., Ed.; Wiley: New York, 1972; Vol. 1 and 2. (b) Wardell, J. L. In Comprehensive Organometallic Chemistry; Wilkinson, G., Stone, F. G. A., Abels, F. W., Eds.; Pergamon: New York, 1982; Vol. 1, Chapter 2. (c) Wakefield, B. J. *The Chemistry of Organolithium Compounds*; Pergamon: New York, 1974. (d) Brown, T. L. *Pure Appl. Chem.* **1970**, *23*, 447.

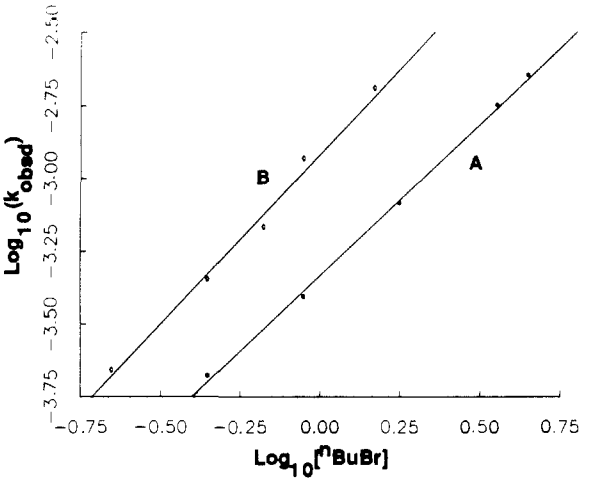

Figure 3. Plots of log (k_{obsd}) vs log [*n*-BuBr] for the alkylation of Ph_2NLi/LiBr (0.015 M) at 51.2 °C. (A) 1.27 M THF, (B) 10.15 M THF.

Table I. First-Order Rate Constants for the Alkylation of Ph_2NLi/LiBr with *n*-BuBr as a Function of THF Concentration[a]

entry	$k_{obsd} \times 10^{-4}$, s^{-1}	[THF], mol/L
1	1.45 ± 0.02	0.19 (1.5%)
2	1.66 ± 0.05	0.44
3	1.74 ± 0.04	0.53
4	1.88 ± 0.02	0.68
5	2.05 ± 0.05	0.97
6	2.11 ± 0.16	1.27
7	2.15 ± 0.05	2.15
8	2.18 ± 0.03	4.37 (35.6%)
9	2.21 ± 0.01	7.33
10	3.00 ± 0.04	8.81
11	3.68 ± 0.08	9.70
12	4.53 ± 0.12	10.15
13	4.98 ± 0.30	10.56
14	6.33 ± 0.27	11.03
15	7.85 ± 0.37	11.55 (94.1%)

[a] 0.015 M Ph_2NLi/LiBr, benzene cosolvent, 0.44 M *n*-BuBr, 51.2 °C. The reported errors represent 1 standard deviation.

Scheme III

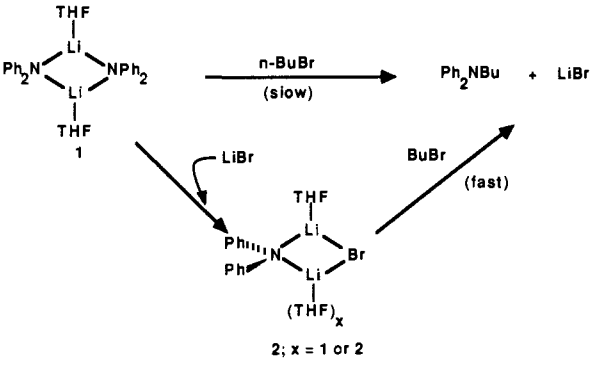

Overall, whether generated during the course of the alkylation or added at the onset, the LiBr causes a substantial rate acceleration. Solution studies described in the preceding paper[13] demonstrate that Ph_2NLi is quantitatively converted to mixed aggregate **2** in the presence of 1.0 equiv of LiBr at low THF concentrations. Thus, by forming mixed aggregate **2**, a more efficient alkylation pathway is made available (Scheme III). Accordingly, we explored the kinetics of amide alkylation in the presence of 1 equiv of LiBr (Ph_2NLi/LiBr). Analysis of the alkylation rates prior to the onset of autocatalysis by LiBr (0–2% conversion) will be discussed later.

Ph_2NLi/LiBr Alkylation: Dependence on *n*-BuBr Concentration. The dependence of the alkylation rate of Ph_2NLi/LiBr on *n*-BuBr concentration was monitored at two different THF concentrations (Figure 3). At low THF concentrations (curve A; 1.27 M THF)

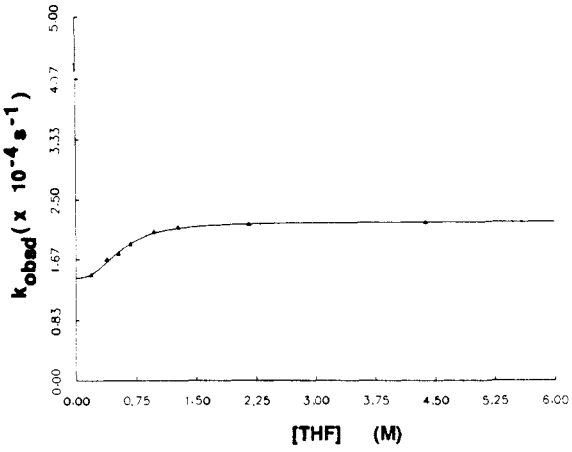

Figure 4. Plot of k_{obsd} vs [THF] for the alkylation of $Ph_2NLi/LiBr$ (0.015 M) by *n*-BuBr (0.44 M) at 51.2 °C. The solid line represents a parametrized fit of the data in Table I (entries 1–9) to eq 1.

Scheme IV

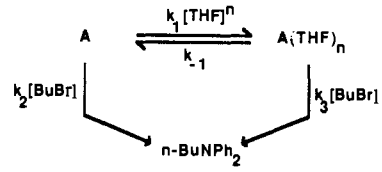

the reaction is first order in *n*-BuBr (calcd 1.05 ± 0.02) over a 10-fold *n*-BuBr concentration range. Although the first-order reaction in *n*-BuBr is also mathematically consistent with rate-determining *n*-BuBr precomplexation, the rates of ligand exchange at lithium are typically many orders of magnitude faster than the reaction in question.[16a,17] In 10.15 M THF (curve B), a slightly higher order (calcd 1.19 ± 0.07) is observed. We believe the deviation from first order stems from very complex solvation effects uncovered in the THF rate dependencies (vide infra). Overall, the alkylation step appears to be rate determining throughout the full range of THF concentrations.

$Ph_2NLi/LiBr$ Alkylation: Dependence on THF Concentration. The rates of the N-alkylation of $Ph_2NLi/LiBr$ as a function of THF concentration are listed in Table I. Rate measurements below 0.19 M THF were precluded by poor solubilities. Alkylations of $Ph_2NLi/LiBr$ in up to 7.33 M THF are first order in amide as evidenced by the linear first-order plots to greater than 4 half-lives. The rate constants beyond 7.33 M THF (60%) were also determined by treating the alkylation as first order in $Ph_2NLi/LiBr$ with the value of k_{obsd} determined from the first 2 half-lives. However, evidence provided below demonstrates that the alkylation rate dependence at high THF concentrations is fractional order rather than first order in $Ph_2NLi/LiBr$ and is further complicated by competing E2 eliminations that require simplifying assumptions. Consequently, the observed rate constants at the high THF concentrations are phenomenological rate constants that reflect macroscopic changes in the observed reaction rate and bear only indirect mechanistic significance.

It is instructive to first focus on the results at low and intermediate THF concentrations. Within the THF concentration range between 0.19 and 7.33 M (17–500 equiv; 1.5–60%), the alkylations measure first order in $Ph_2NLi/LiBr$ to greater than 95% conversion (>4 half-lives). A plot of k_{obsd} versus THF concentration appears in Figure 4 along with a numerical fit to eq 1.

It proves most convenient to discuss the THF dependence plotted in Figure 4 in the context of the generic mechanism and rate expression depicted in Scheme IV and eq 1 ($K_{eq} = k_1/k_{-1}$; $[A_T]$ = total Ph_2NLi concentration). While such a scheme reflects

Scheme V

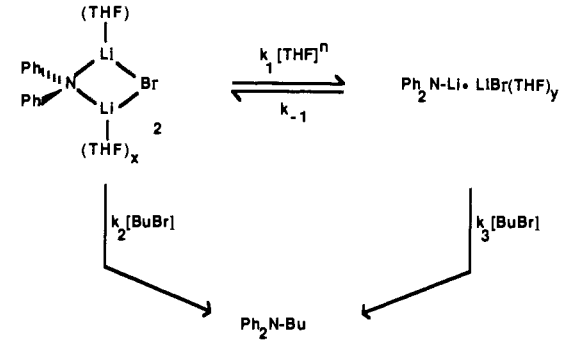

Scheme VI

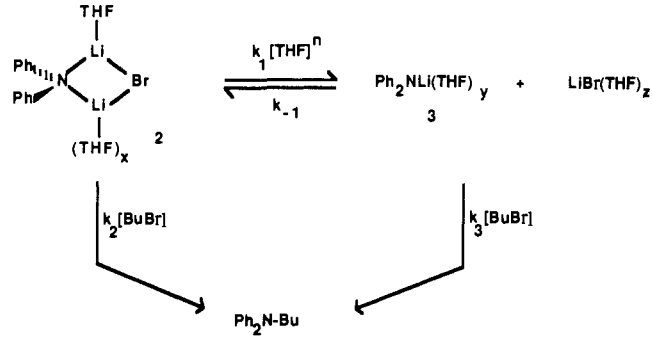

the limiting behaviors anticipated in a solvent-dependent equilibrium, it is simplified to the extent that it ignores the possibility that the more solvated form depicted as $A(THF)_n$ could correspond to a dissociated species (vide infra). In the case of such a dissociation, the rate equation would take on a more complex mathematical form, showing first-order dependencies on the organolithium concentration at the two limiting extremes and fractional orders in the fall-off region near the inflection point (cf. Figure 4).[18] However, since superior quality experimental data would be required to distinguish dissociative and nondissociative equilibria, the simplified kinetic model is adequate.

In the limit of very low THF concentrations, eq 1 reduces to eq 2 with the measured value of k_{obsd} corresponding to $k_2[n\text{-BuBr}]$. The nonzero *y* intercept in Figure 4 corresponds to the alkylation of a species of low solvation number requiring no additional solvation. (Although the data depicted in Figure 4 supporting such a nonzero *y* intercept are inconclusive, additional evidence comes from studies using cosolvents other than benzene, vide infra.) The region in which the rate is a function of THF concentration is indicative of the increasing importance of a new pathway proceeding via a more highly solvated reactive intermediate ($A(THF)_n$). At sufficiently high THF concentrations, the equilibrium shifts to produce $A(THF)_n$ as the predominant species; the rate again levels out showing no further dependence on the THF concentration. In the high THF concentration limit, eq 1 reduces to eq 3 with k_{obsd} corresponding to $k_3[n\text{-BuBr}]$.

$$d[Ph_2NBu]/dt = \frac{k_2 + k_3 K_{eq}[THF]^n}{1 + K_{eq}[THF]^n}[A_T][BuBr] \quad (1)$$

$$d[Ph_2NBu]/dt = k_2[A][BuBr] \quad (2)$$

$$d[Ph_2NBu]/dt = k_3[A][BuBr] \quad (3)$$

In principle, the observed saturation kinetic behavior is consistent with either of the two mechanisms shown in Schemes V and VI. Nevertheless, cogent arguments can be made in support of the dissociative pathway in Scheme VI. Evidence cited in the previous manuscript indicates that both dimeric Ph_2NLi and mixed dimer Ph_2NLi·LiBr dissociate to a common Ph_2NLi monomer as

(17) Organolithium–electrophile precomplexation has been detected: Al-Aseer, M.; Beak, P.; Hay, D.; Kempf, D. J.; Mills, S.; Smith, S. G. *J. Am. Chem. Soc.* **1983**, *105*, 2080. Meyers, A. I.; Rieker, W. F.; Fuentes, L. M. *J. Am. Chem. Soc.* **1983**, *105*, 2082.

(18) Müller, A. H. E. In *Recent Advances in Anionic Polymerization*; Hogen-Esch, T. E., Smid, J., Eds.; New York, 1987; p 205.

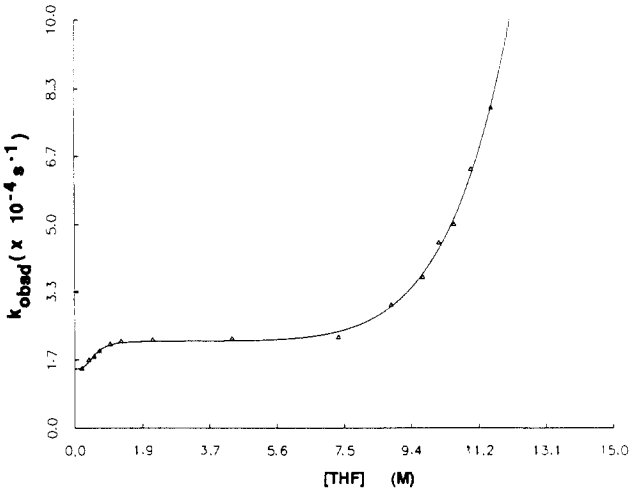

Figure 5. Plot of k_{obsd} vs [THF] for the alkylation of $Ph_2NLi/LiBr$ (0.015 M). The solid line represents a parametrized numerical fit of the data in Table I to eq 4.

the THF concentrations are increased. Secondly, the dramatic induction periods observed at low THF concentrations (Figure 1) disappear at the intermediate and high THF concentrations—the same concentrations that the alkylation rate levels off to zero order in THF. (Spectroscopic and rate data must be compared cautiously, however, because of the dramatically different temperatures of the two measurements.) Lastly, rate studies of Ph_2NLi at early conversion (vide infra) further demonstrate that the alkylation rates of Ph_2NLi in the absence of LiBr and $Ph_2NLi/LiBr$ mixtures are indistinguishable at elevated THF concentrations. Overall, the failure of the LiBr to influence either the spectroscopic properties or alkylation rates of Ph_2NLi at the higher THF concentrations argues against the intermediacy of any form of Ph_2NLi·LiBr mixed aggregate.

Since the colligative and spectroscopic studies indicate that **2** is predominantly trisolvated (**2a**) at 0.2 M concentration and 0 °C,[13] we can estimate that at the decreased $Ph_2NLi/LiBr$ concentration and elevated temperature of the kinetic analysis the mixed aggregate undergoing N-alkylation at the low THF concentration limit is at most tri- (and possible di-) solvated. Although the numerical fit could, in principle, afford the number of solvents required to attain the more highly solvated species, the quality of the data and the complexity of the fit do not warrant such an extrapolation.

The autocatalysis by LiBr at low THF concentrations appears to stem from a dramatically increased rate of alkylation of Ph_2NLi·LiBr relative to the parent Ph_2NLi dimer. This rate difference presumably derives, at least in part, from the decreased steric demands of a bromide ion. The reasons that the mixed aggregate and monomer are so close in reactivity (despite the absence of lone pairs on the nitrogen nucleus of the mixed aggregate) is not at all clear at this time.

$Ph_2NLi/LiBr$ Alkylation: High THF Concentrations. As the THF concentrations exceed 7.33 M (60%), the extended region of zero-order THF dependence is followed by a sudden exponential dependence, indicating the appearance of a new mechanistic pathway with a large solvation requirement (Figure 5). Numerical fit of the rate data listed in Table I to eq 4 demonstrates

$$d[Ph_2NBu]/dt = \left[\frac{k_2 + k_3 K_{eq}[THF]^n}{1 + K_{eq}[THF]^n} + k'[THF]^m\right][BuBr][A_T] \quad (4)$$

the alkylation rate to increase in proportion to the *seventh* power of the THF concentration ($m = 7.03 \pm 0.01$).[19] Alternative numerical fits of the rate data at elevated THF concentrations using simplified or linearized expressions afford similar high orders within ±0.5.

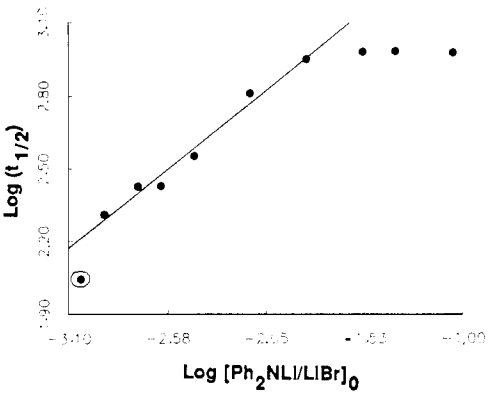

Figure 6. Plot of log ($t_{1/2}$) vs log $[Ph_2NLi/LiBr]_0$ to determine reaction order in $Ph_2NLi/LiBr$ in neat THF. The circled data point was not included in the fit; inclusion of it yielded an order of 0.32 ± 0.07.

Further studies of the alkylation rate as a function of the $Ph_2NLi/LiBr$ concentration, medium polarity, and added lithium salts described below clarify the origins of the high THF dependence.

$Ph_2NLi/LiBr$ Alkylation: Dependence on $Ph_2NLi/LiBr$ Concentration. Throughout the low and intermediate THF concentration range, the alkylation rates display first-order dependencies on the $Ph_2NLi/LiBr$ concentration. However, at elevated THF concentrations the competing elimination to form 1-butene causes substantial upward curvatures in the first-order plots (cf. Figure 1, curve c) that obscure any downward curvatures resulting from a fractional-order dependence of a dissociative alkylation pathway.[16] Indeed, the measured rate constants (monitored to 1 half-life) increase markedly as the initial concentrations of $Ph_2NLi/LiBr$ are decreased. The reaction order in amide can be determined by using the Noyes equation[20] (eq 5), where n is

$$\log(t_{1/2}) = C + (n-1)\log[A_0] \quad (5)$$

the calculated order in species A, $[A_0]$ is the initial concentration of A, and $t_{1/2}$ is the calculated half-life. A plot of log ($t_{1/2}$) vs log $[Ph_2NLi/LiBr_0]$ shows two distinct linear regions with slopes corresponding to $1 - n$ (Figure 6). Linear fit to eq 5 from rate constants measured over a 12-fold decrease in initial $Ph_2NLi/LiBr$ concentrations provides a calculated order, n, of 0.39 ± 0.04. Such a fractional order is characteristic of some form of dissociative preequilibrium. At elevated $Ph_2NLi/LiBr$ concentrations, k_{obsd} rapidly tapers off to a constant value independent of $Ph_2NLi/LiBr$ concentration. This would correspond to the limiting case in which the high $Ph_2NLi/LiBr$ concentrations inhibit the dissociative pathway and the reaction rate derives predominantly from the first-order, nondissociative (monomer) alkylation described previously.

$Ph_2NLi/LiBr$ Alkylation: Dependence on Dielectric Properties. The systematic increases in the THF concentrations at the expense of the inert cosolvent (benzene) inadvertently cause increases in the dielectric properties of the medium as well as changes in the nature of solvent–solvent interactions. To determine the extent that these secondary effects contribute to the measured seventh-order THF dependence, the alkylation rates were monitored in several different cosolvents.

The absence of anomalous rate effects due to solvent–solvent or solvent–lithium interactions arising from the π system of benzene[21] is confirmed by the absence of a measurable change in the alkylation rate (<3%) with cyclohexane as the cosolvent.

(19) The calculated values of the adjustable parameters were as follows. Figure 4 (eq 1): $k_2 = 1.41 \pm 0.02$, $k_3 = 4.21 \pm 0.32$, $K_{eq} = 2.18 \pm 0.01$, $n = 2.51 \pm 0.12$; Figure 5 (equation 4): $k_2 = 1.44 \pm 0.08$, $k_3 = 6.80 \pm 0.03$, $K_{eq} = 2.12 \pm 0.03$, $n = 3.15 \pm 0.60$, $k' = 1.86 \pm 0.02 \times 10^{-7}$, $m = 7.03 \pm 0.01$.

(20) Casado, J.; Lopez-Quintela, M. A.; Lorenzo-Barral, F. M. *J. Chem. Educ.* **1986**, *63*, 450. Moore, J. W.; Pearson, R. G. *Kinetics and Mechanism*, 3rd ed.; Wiley: New York, 1981; Chapter 3. Hammes, G. G. *Principles of Chemical Kinetics*; Academic: New York, 1978; pp 14–15.
(21) Jutzi, P. *Adv. Organomet. Chem.* **1986**, *26*, 217.

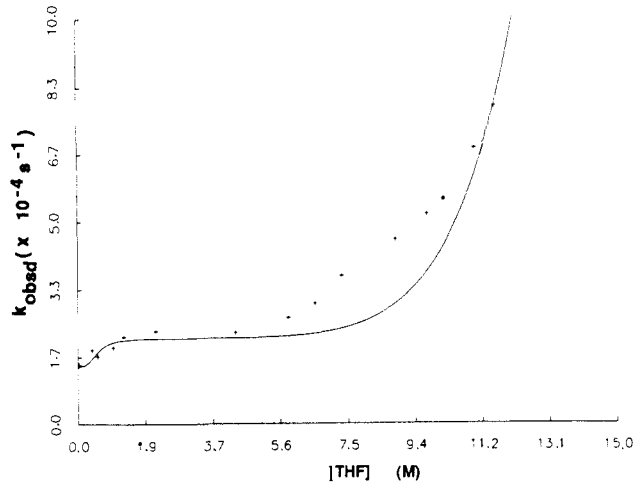

Figure 7. Plot of k_{obsd} vs [THF] for the alkylation of Ph_2NLi/LiBr (0.015 M) by *n*-BuBr (0.44 M) in THF/Me_2THF mixtures. The (+) symbols represent data from THF/Me_2THF mixtures. The solid line is the numerical fit from THF/benzene mixtures abstracted from Figure 5.

The influence of the dielectric properties of the medium was investigated with 2,5-dimethyltetrahydrofuran (Me_2THF) as the cosolvent. The steric hinderance about the oxygen of Me_2THF has been found to decrease its donor capabilities by as much as a factor of 200 relative to THF,[22] while the dielectric constant can be estimated to be only slightly lower than that of THF.[23] A plot of k_{obsd} vs [THF] in Me_2THF cosolvent is illustrated in Figure 7. The solid curve represents the fitted function from the THF/benzene mixtures abstracted from Figure 5 and superimposed for comparison. Alkylation rates in THF/Me_4THF mixtures (Me_4THF = 2,2,5,5-tetramethyltetrahydrofuran) measure within 3% of rates in comparable THF/Me_2THF mixtures.

The observed N-alkylation rates at low THF concentrations clearly show a minimal dependence on the dielectric properties. Because of improved solubility, the nonzero *y* intercept corresponding to the alkylation rate in the absence of uncoordinated THF was directly measured and is within 2% of the calculated value for the THF/benzene mixtures. The only noticeable effect of maintaining a medium of high dielectric strength throughout the entire THF concentration range is the appearance of the dissociative pathway at intermediate THF concentrations.

Fitting the rate data from the THF/Me_2THF mixtures to eq 4 affords calculated THF orders of 4–6, depending on the fitting procedural details. Hence, we can only qualitatively note that dielectric effects account for a significant yet minor portion of the measured THF rate dependence. The rate increases that occur upon replacement of benzene with sterically hindered Me_2THF and Me_4THF must be quite long range. In contrast, rate changes that occur upon increasing the THF concentration in THF/Me_2THF mixtures do not include substantial dielectric contributions and, thus, appear to derive from sterically dependent solvation not available to the more hindered methylated tetrahydrofurans. We do not believe, however, that such sterically dependent solvation effects necessarily arise from direct interaction of the donor with lithium nuclei. We will return to this point in the Discussion Section.

Ph_2NLi/LiBr Alkylation: Dependence on Added Lithium Salts. At low THF concentrations, linear first-order plots show no evidence of inhibition or catalysis by the second equivalent of LiBr generated during the course of the alkylation. This is further reflected by the relative insensitivity of the reaction rate to greater than 1.0 equiv of LiBr added at the onset, as well as to added $LiClO_4$ and $LiBPh_4$ (Table II).[24,25] These results are fully consistent with alkylation mechanisms involving direct alkylation of the predominant species in solution as discussed previously (Scheme VI).

Table II. Observed Rate Constants for the Alkylation of Ph_2NLi/LiBr with *n*-BuBr as a Function of Added Lithium Salts[a]

entry	$k_{obsd} \times 10^{-4}$, s^{-1}	[THF], mol/L	additive, mol/L
1	2.18 ± 0.03	4.37 (35.6%)	
2	2.34 ± 0.06	4.37	LiBr,[b] 0.044
3	2.23 ± 0.01	4.37	$LiClO_4$, 0.015
4	2.24 ± 0.10	4.37	$LiBPh_4$, 0.015
5	4.53 ± 0.12	10.15 (82.7%)	
6	4.66 ± 0.14	10.15	LiBr,[b] 0.044
7	3.55 ± 0.04	10.15	$LiClO_4$, 0.015
8	2.93 ± 0.02	10.15	$LiBPh_4$, 0.015

[a] 0.015 M Ph_2NLi/LiBr, 0.44 M *n*-BuBr, 51.2 °C. The reported errors represent 1 standard deviation. [b] 0.044 equiv of LiBr in addition to the 0.015 mmol of LiBr added to prepare the Ph_2NLi/LiBr (1:1) mixture.

Scheme VII

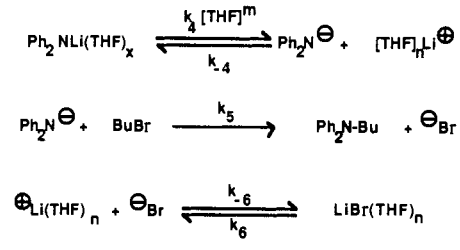

In the high THF limit wherein a significant contribution of the highly solvent-dependent dissociative pathway can be detected, inhibitions by an additional equivalent of LiBr, $LiClO_4$, and $LiBPh_4$ of 2%, 42%, and 68% (respectively) are observed. The magnitude of the inhibitions qualitatively match the relative magnitudes of their free-ion dissociation constants (K_{diss}) in aprotic, nonpolar solvents.[26-29] In light of the measured fractional order in Ph_2NLi, the high order in THF, and the appreciable dependence of the rate on the dielectric strength of the medium, we attribute the effects of the added lithium salts to common ion rate inhibition of an alkylation pathway proceeding via free lithium ions. If the predominant solution species at the elevated THF concentrations

(22) Gutmann, V. *The Donor–Acceptor Approach to Molecular Interactions*; Plenum: New York, 1978. Chan, L. L.; Smid, J. *J. Am. Chem. Soc.* **1968**, *90*, 4654.

(23) The dielectric constants of substituted tetrahydrofurans are slightly lower than THF. Harada, Y.; Salomon, M.; Petrucci, S. *J. Phys. Chem.* **1985**, *89*, 2006. Carvajal, C.; Tolle, K. J.; Smid, J.; Szwarc, M. *J. Am. Chem. Soc.* **1965**, *87*, 5548.

(24) Although the reproducible 8% increase in rate observed upon addition of 4 equiv of LiBr (Table III, entry 1) could be indicative of electrophilic catalysis (ref 25), this would seem unlikely in light of the minimal effects of $LiClO_4$ and $LIBPh_4$.

(25) Jackman, L. M.; Dunne, T. S. *J. Am. Chem. Soc.* **1985**, *107*, 2805. Pierre, J.-L.; Handel, H. *Tetrahedron Lett.* **1974**, 2317. Loupy, A.; Seyden-Penne, J.; Tchoubar, B. *Tetrahedron Lett.* **1976**, 1677. Buncel, E.; Dunn, E. J.; Bannard, R. A. B.; Purdon, J. G. *J. Chem. Soc., Chem. Commun.* **1984**, 162. Chang, C. J.; Kiesel, R. F.; Hogen-Esch, T. L. *J. Am. Chem. Soc.* **1973**, *95*, 8446. Loupy, A.; Seyden-Penne, J. *Tetrahedron* **1980**, *36*, 1937.

(26) Physicochemical studies of lithium electrolytes in THF: Pocker, Y.; Buchholz, R. F. *J. Am. Chem. Soc.* **1970**, *92*, 2075. Edgell, W.; Lyford, J.; Wright, R.; Resin, W.; Watts, A. *J. Am. Chem. Soc.* **1970**, *92*, 2240. Day, M. C. *Pure Appl. Chem.* **1977**, *49*, 75. Maaser, H.; Xu, M.; Hemmes, P.; Petrucci, S. *J. Phys. Chem.* **1987**, *91*, 3047. Abraham, K. M. *J. Power Sources* **1985**, *14*, 179. Braun, R.; Sauer, J. *Chem. Ber.* **1986**, *119*, 1269. Saar, D.; Petrucci, S. *J. Phys. Chem.* **1986**, *90*, 3326.

(27) Physicochemical studies of $LiClO_4$ in THF, substituted THF's, and THF/benzene mixtures: Badiali, J.-P.; Cachet, H.; Cyrot, A.; Lestrade, J.-C. *J. Chem. Soc., Faraday Trans.* **1973**, *69*, 1339. Cachet, H.; Cyrot, A.; Fekir, M.; Lestrade, J.-C. *J. Phys. Chem.* **1979**, *83*, 2419. Ashby, E. C.; Dobbs, F. R.; Hopkins, H. P., Jr. *J. Am. Chem. Soc.* **1973**, *95*, 2823. Matsuda, Y.; Morita, M.; Tachihara, F. *Bull. Chem. Soc. Jpn.* **1986**, *59*, 1967. Delsignore, M.; Maaser, H. E.; Petrucci, S. *J. Phys. Chem.* **1984**, *88*, 2405. Tobishima, S.; Yamaji, A. *Electrochim. Acta* **1983**, *28*, 1067.

(28) LiCl and LiBr appear to form higher aggregates in THF and THF/benzene mixtures: Goralski, P.; Chabanel, M. *Inorg. Chem.* **1987**, *26*, 2169 and references cited therein.

(29) Physicochemical studies of $LiBPh_4$ in THF: Bhattacharyya, D. N.; Lee, C. L.; Smid, J.; Szwarc, M. *J. Phys. Chem.* **1965**, *69*, 608. Wong, M. K.; Popov, A. I. *J. Inorg. Nucl. Chem.* **1972**, *34*, 3615.

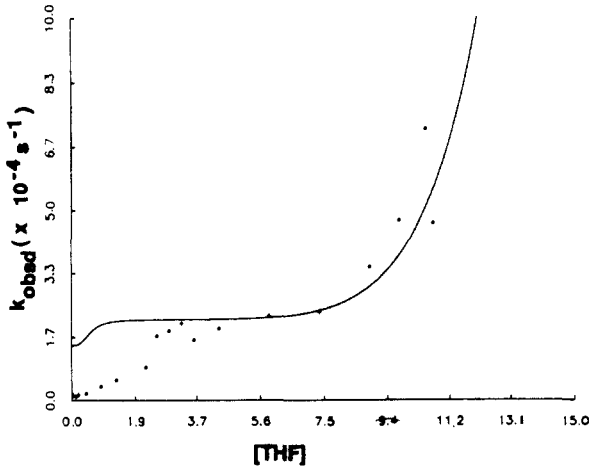

Figure 8. Plot of k_{obsd} vs [THF] for the alkylation of Ph_2NLi (0.015 molar) by *n*-BuBr (0.44 M) at 51.2 °C monitored to 2% conversion. The solid line depicts results from Ph_2NLi/LiBr mixtures abstracted from Figure 5 and superimposed for comparison.

is indeed some form of monomer uncomplexed by LiBr as described previously,[13] then the dissociative ionization can be depicted as shown in Scheme VII and eq 6.[30]

$$d[Ph_2NBu]/dt = \frac{k_4k_5[BuBr]}{k_{-4}[Li^+] + k_5[BuBr]}[Ph_2N^{\ominus}][THF]^m \quad (6)$$

$$d[Ph_2NBu]/dt = \frac{k_4k_5[BuBr][Ph_2N^{\ominus}][THF]^m}{k_{-4}[Li^+]} \quad (7)$$

$$XLi(THF)_n \underset{k_{-7}}{\overset{k_7}{\rightleftharpoons}} \oplus_{Li(THF)_n} + \ominus X \quad (8)$$

Since ion–ion recombinations approach diffusion controlled rates and are surely rapid relative to the rate of alkylation[31] (as required by the measured first-order *n*-BuBr dependence), $k_{-4}[Li^+] \gg k_5[BuBr]$, and the rate expression simplifies to eq 7. The common ion rate inhibitions would arise from an increase in free lithium ion concentration according to eq 8. If so, then there are three possible outcomes: (1) In the event that K_{diss} of the added lithium salt is much less than the K_{diss} of Ph_2NLi, the concentration of Li^+ ions would not be appreciably increased by the added salt and no inhibition would be observed. (2) If K_{diss} of the added salt is very large relative to K_{diss} of Ph_2NLi, efficient rate inhibition would occur. The only contribution to the alkylation rate would come from the nondissociative pathways. (3) If the K_{diss}'s of the added salt and Ph_2NLi are approximately equal, then partial, salt-dependent inhibition of the ionization pathway would be observed.[32]

The magnitudes of the rate inhibitions indicate that the K_{diss} of Ph_2NLi is larger than K_{diss} of LiBr (case 1) and comparable to the values for $LiClO_4$ and $LiBPh_4$ (case 3). This is initially surprising given the far greater basicity of the Ph_2N^- fragment in comparison to the other gegenions. It has been noted, however, that the free-ion dissociation constants of *solvent-separated ion pairs* (but not contact ion pairs) are relatively insensitive to the structure of the anionic counterion and highly sensitive to the dielectric properties of the medium.[33] Thus, our results are reconcilable with a free ion mechanism *if* the predominant solution structures of Ph_2NLi, $LiBPh_4$, and $LiClO_4$ in THF are solvent-separated ion pairs and LiBr is a contact ion pair. Studies of the latter three species in nonaqueous solvents are congruent with this proposition.[26-29]

Table III. Substitution/Elimination Selectivities in the Reaction of Ph_2NLi/LiBr with *n*-Octyl Bromide[a]

entry	[THF], mol/L	additive, mol/L	subst/elim
1	7.33[b] (59.7%)		96:2
2	8.81[b]		92:8
3	9.70[b]		92:8
4	10.15[b]		90:10
5	10.56[b]		89:11
6	11.03[b]		88:12
7	11.55[b] (94.1%)		87:13
8	11.55	HMPA, 0.06	85:15
9		DME, 8.94	90:10
10		Et_2O, 8.85	99:1
11	11.15[c]		98:2
12	11.30	$LiBPh_4$, 0.015	35:65

[a] 0.015 M in Ph_2NLi/LiBr, 0.44 M *n*-octyl bromide; 51.2 °C. [b] Benzene cosolvent. [c] 0.045 M in Ph_2NLi/LiBr, 0.44 M *n*-octyl bromide; 51.2 °C.

Ph_2NLi Alkylation: Kinetics at Early Conversion. To place the alkylation rates of the Ph_2NLi·LiBr mixed aggregate and the role of autocatalysis by LiBr in the context of the alkylation of Ph_2NLi in the absence of LiBr, we investigated the rate of alkylation prior to the onset of autocatalysis. Since the curvature in the first-order plots appear as early as 5% conversion, the rates were monitored up to only 2% conversion. A plot of k_{obsd} vs THF concentration is illustrated in Figure 8. The solid line represents the fitted function for Ph_2NLi/LiBr alkylations abstracted from Figure 5 for comparison.

The substantial error in the initial rate determinations precludes all but a low-resolution view of the THF rate dependencies of the alkylation in the absence of LiBr. There are, however, several features of the data that should be noted. At very low THF concentrations (0.01–0.87 M) the initial alkylation rates are approximately 1 order of magnitude lower than the rates for the corresponding Ph_2NLi·LiBr mixed aggregate. Secondly, in the preliminary probes of the alkylation rate without added LiBr (Figure 1), the autocatalysis by LiBr is absent at the intermediate and high THF concentrations. This is reflected in the initial rate measurements. These results provide further support to the contention that the LiBr and Ph_2NLi do not associate at elevated THF concentrations and that the alkylation at intermediate THF concentration occurs via a monomeric amide intermediate according to Scheme VI.

On the Elimination/Substitution Selectivity. We are now in a position to place the carbon- and proton-centered nucleophilicity of Ph_2NLi/LiBr in a mechanistic context. Ph_2NLi/LiBr showed >98% selectivity for substitution with primary alkyl bromides at low and intermediate THF concentrations and a propensity to partition between elimination and substitution pathways at high THF concentrations (Scheme I). Because of analytical problems, we were forced to study the substitution/elimination selectivity using *n*-octyl bromide rather than *n*-butyl bromide (Table III).

The S_N2/E2 branching ratio appears to reach a limiting value of approximately 87/13 favoring substitution in THF/benzene mixtures. Despite the change in the alkyl bromide and a number of other systematic errors,[34] the elimination products coincide qualitatively with the increasing importance of the free-ion pathway. If indeed the elimination proceeds via a free ion intermediate that partitions with an approximate 87/13 substitu-

(30) The model depicted in Scheme VI depends critically on the assignment of the predominant form of Ph_2NLi as *uncomplexed* by LiBr. If, indeed, the assignment is not correct and Ph_2NLi/LiBr mixtures at elevated THF concentrations contain appreciable concentrations of mixed aggregates, then the observed common-ion inhibition, fractional-order, and dielectric dependencies could be interpreted in the context of other dissociations and ionizations. Conductivity studies by Streitwieser and co-workers should shed light on this issue.

(31) Harada, Y.; Salomon, M.; Petrucci, S. *J. Phys. Chem.* **1985**, *89*, 2006.

(32) For the details of a more quantitative treatment of common lithium ion inhibition, see Gronert, S.; Streitwieser, A., Jr. *J. Am. Chem. Soc.* **1988**, *110*, 2836.

(33) A particularly startling example is the approximately equal dissociation constants for the living end of polystyrene (polymer-CH(Na)Ph) and $NaBPh_4$ in THF. Bhattacharyya, D. N.; Lee, C. L.; Smid, J.; Szwarc, M. *J. Phys. Chem.* **1965**, *69*, 612. See also, Streitwieser, A., Jr. *J. Phys. Chem.* **1964**, *68*, 2922. Kaufmann, M. J.; Gronert, S.; Streitwieser, A., Jr. *J. Am. Chem. Soc.* **1988**, *110*, 2829.

(34) The ratios of alkylation vs elimination were measured at complete conversion and thus do not include changes as a function of percent conversion.

tion/elimination selectivity, then one would predict: (1) an increase in the percent alkylation with increasing amide concentration (due to the *relatively* larger contribution from the nondissociative alkylation pathway) and (2) a dramatic increase in alkylation rate in highly polar aprotic solvents *without* concomitant substantial change in the branching ratio. Indeed, the elimination pathway is almost totally shut down by a threefold increase in $Ph_2NLi/LiBr$ concentration (Table III entry 11). Additionally, alkylation of $Ph_2NLi/LiBr$ in neat THF containing 4 equiv of HMPA proceeded at an estimated 10^2–10^3 increased rate[35] while showing a branching ratio of 85:15.

The situation is not totally straightforward, however. One would also expect that added $LiBPh_4$ should inhibit the dissociative alkylation and elimination pathways, causing a net increase in the observed percent alkylation arising from the unaffected nondissociative alkylation pathway. On the contrary, $LiBPh_4$ causes a reproducible *decrease* in the percentage of the alkylation product (Table III, entry 12). While one might surmise that electrophilic catalysis by the lithium ion[25] could preferentially enhance the rate of the elimination pathway to produce such a result, additional experiments are required to clarify the details.[36]

Discussion

Summary. During the course of studies of the N-alkylation reaction of lithium diphenylamide with *n*-butyl bromide, a number of kinetically active species were detected as summarized in Scheme II.

At very low THF concentrations, di- or trisolvated dimeric Ph_2NLi (**1**) are shown to be the predominant solution species by ^6Li, ^{13}C, and ^{15}N NMR spectroscopy and colligative measurements.[13] Dramatic induction periods were traced to the conversion of dimer **1** to the substantially more reactive mixed aggregate **2**.

As the THF concentrations are systematically increased, alkylation rates of $Ph_2NLi/LiBr$ mixtures show a distinct THF concentration dependence, indicating the contribution from a pathway involving a more highly solvated intermediate. At intermediate THF concentrations the equilibrium shifts toward the more highly solvated species, and the rate becomes THF concentration-independent (Figure 2). We considered two mechanistic scenarios corresponding to: (1) alkylation of a more highly solvated mixed aggregate (Scheme V) and (2) alkylation of the Ph_2NLi monomer (Scheme VI). Although neither mechanism can be rigorously excluded, disappearance of the influence of the LiBr on the reactivity and spectroscopic properties of Ph_2NLi is most consistent with direct alkylation of monomer (or ion pair) **3** at intermediate THF concentrations.

At THF concentrations above the range showing THF-concentration-independent reaction rates, the alkylation rate rises sharply with increasing THF concentration (Figure 5). This additional solvent-dependent pathway exhibits rates proportional to the *seventh power* of the THF concentration and a number of properties not apparent at the lower THF concentrations. Whereas the rates of alkylation at low and intermediate THF concentrations are relatively unaffected by added lithium salts or changes in the dielectric properties of the medium, at high THF concentrations the rates are markedly decreased by added $LiBPh_4$ and $LiClO_4$ and increased by polar cosolvents such as 2,5-dimethyltetrahydrofuran and 2,2,5,5-tetramethyltetrahydrofuran. In addition, at low and intermediate THF concentrations the rates exhibit first-order dependencies on the $Ph_2NLi/LiBr$ concentration; a significant fractional amide order is observed at high THF concentrations. From these observations, we ascribe the explosive increase in alkylation rate to a pathway involving free ions (Scheme VII).

As the free ion alkylation pathway becomes a major contributor to the observed alkylation rate, elimination to give alkene becomes a substantial side reaction. The qualitative correspondence between free-ion intermediates and elimination products was investigated by monitoring the effects of highly polar solvents and lithium salt additives on the substitution/elimination branching ratios.

On the Role of Mixed Aggregates and Autocatalysis. The effects of lithium halides and lithium alkoxides on the reactivities and selectivities of organolithium compounds have been noted on a number of occasions.[3,5,37-43] Although mixed aggregates have been detected spectroscopically[16,37-39] and crystallographically,[40,41] for the most part their roles as reactive entities are poorly understood.[39,42,43] This represents a serious conceptual gap in our understanding of organolithium chemistry since, by definition, all organolithium reactions generate lithium-containing byproducts capable of altering the reaction mechanism in situ.

In the context of lithium amides, Fraser has noted a modest inhibiting effect of added LiBr on the kinetic basicity of lithium amides.[2] Seebach and Polt very recently reported important effects of LiBr and LiCl on the selectivities of enolizations mediated by lithium diisopropylamide.[44] The reactivities and selectivities of many of the in situ trapping mixtures showing increased popularity very recently (e.g. R_2NLi/Me_3SiCl) possibly are influenced by the LiCl generated during the course of the reactions.[45] However, of the documented mixed aggregation effects, we draw specific attention to the studies of Huisgen and co-workers[6] on the dehydrohalogenations of aryl halides with lithium piperidide (eq 9).

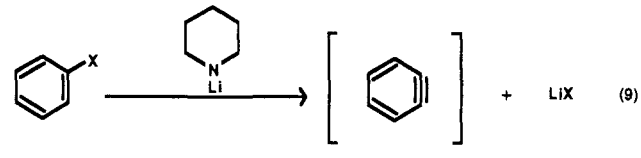

During the course of rate studies, an autoinhibition by lithium halides was detected and is attributed to the formation of mixed aggregates analogous to **2**. To understand why the intervention of (presumably) structurally analogous mixed aggregates have an inhibiting effect on one reaction and a promoting effect on

(35) The rate increase was estimated from rate measurements made at 0 °C. The branching ratio was measured at 51 °C.

(36) Pierre and co-workers observed a sixfold rate enhancement in the alkylation of $Ph_2NK/C[2.2.2]$ (1:1) in THF with *n*-pentyl bromide relative to cryptand-free conditions, no elimination was detected. Pierre, J. L.; Goaller, R. Le; Pasquini, M. A. *Tetrahedron* **1980**, *36*, 1223. However, recently completed studies on the structures and reactivities of cryptates of lithiated and natriated hydrazones reveal that the chemistry of cryptates derived from highly reactive organolithium derivatives can be exceedingly complex. Galiano-Roth, A. S.; Collum, D. B. *J. Am. Chem. Soc.* **1980**, *110*, 3546.

(37) van Rijn, P. E.; Mommers, S.; Visser, R. G.; Verkruijsse, H. D. *Synthesis* **1981**, 459. Waack, R.; Doran, M. A. *Chem. Ind.* **1964**, 496. Reich, H.; Eisenhart, E. K.; Olson, R. E.; Kelly, M. J. *J. Am. Chem. Soc.* **1986**, *108*, 7791. Maryanoff, B. E.; Reitz, A. B.; Mutter, M. S.; Inners, R. R.; Almond, H. R., Jr.; Whittle, R. R.; Olofson, R. A. *J. Am. Chem. Soc.* **1986**, *108*, 7664.

(38) Jackman, L. M.; Lange, B. C. *Tetrahedron* **1977**, *33*, 2737.

(39) Jackman, L. M.; Dunne, T. S. *J. Am. Chem. Soc.* **1985**, *107*, 2805. Jackman, L. M.; Szevernyi, N. M. *J. Am. Chem. Soc.* **1977**, *99*, 4954. McGarrity, J. F.; Ogle, C. A.; Brich, Z.; Loosli, H.-R. *J. Am. Chem. Soc.* **1985**, *107*, 1810. McGarrity, J. F.; Ogle, C. A. *J. Am. Chem. Soc.* **1985**, *107*, 1805. Holm, T. *Acta Chem. Scand.* **1969**, *23*, 1829. Smith, S. G.; Charbonneau, L. F.; Novak, D. B.; Brown, T. L. *J. Am. Chem. Soc.* **1972**, *94*, 7059. Eppley, R. L.; Dixon, J. A. *J. Am. Chem. Soc.* **1968**, *90*, 1606. Al-Aseer, M. A.; Allison, B. D.; Smith, S. G. *J. Org. Chem.* **1985**, *50*, 2715.

(40) Setzer, W. N.; Schleyer, P. v. R. *Adv. Organomet. Chem.* **1985**, *24*, 354.

(41) Williard and Hintze recently reported the X-ray crystal structure of an enolate–LDA mixed aggregate: Williard, P. G.; Hintze, M. J. *J. Am. Chem. Soc.* **1987**, *109*, 5539.

(42) The effects of alkoxides on rates of anionic olefin polymerization has been well documented: Cubbon, R. C. P.; Margerison, D. *Prog. React. Kinet.* **1965**, *3*, 403. Szwarc, M. *Carbanions, Living Polymers, and Electron Transfer Processes*; Interscience: New York, 1968. Roovers, J. E. L.; Bywater, S. *Macromolecules* **1968**, *1*, 328.

(43) Seebach, D. In *Proceedings of the Robert A. Welch Foundation Conferences on Chemistry and Biochemistry*; Wiley: New York, 1984; p 93.

(44) Polt, R.; Seebach, D. *Helv. Chim. Acta* **1987**, *70*, 1930.

(45) Corey, E. J.; Gross, A. W. *Tetrahedron Lett.* **1984**, *25*, 495. Taylor, S. L.; Lee, D. Y.; Martin, J. C. *J. Org. Chem.* **1983**, *48*, 4156. Marsai, F.; Laperdrix, B.; Güngör, T.; Mallet, M.; Queguiner. G. *J. Chem. Res., Miniprint* **1982**, 2863. Krizan, T. D.; Martin, J. C. *J. Am. Chem. Soc.* **1983**, *105*, 6155. Eaton, P. E.; Castaldi, G. *J. Am. Chem. Soc.* **1985**, *107*, 724. Eaton, P. E.; Cunkle, G. T.; Marchioro, G.; Martin, R. M. *J. Am. Chem. Soc.* **1987**, *109*, 948. Tobia, D.; Rickborn, B. *J. Org. Chem.* **1986**, *51*, 3849. Mirsadeghi, S.; Rickborn, B. *J. Org. Chem.* **1986**, *51*, 986.

another, one must note the differences in the two reactions.

From the work described herein, it appears that the dehydrohalogenations proceed most readily via an ionization pathway and sluggishly (if at all) from aggregated amides. If so, then the mixed aggregate formation with lithium halides represents a form of competitive inhibition, in which formation of a thermodynamically stable adduct decreases the propensity of a lithium amide to ionize (principle of detailed balance[20]). In contrast, the N-alkylation of Ph_2NLi appears to occur with reasonable efficacy on an aggregate framework. The observed autocatalysis derives from the facile alkylation of such mixed aggregates relative to their homonuclear dimer counterparts.

Furthermore, the N-alkylation of Ph_2NLi via the ionization pathway is unaffected by LiBr. Presumably the aromatic rings impart electronic stabilization to the sterically hindered amide fragment, thereby causing the free-ion dissociation constant of Ph_2NLi to be large relative to that of LiBr. Lithium piperidide, on the other hand, lacks such electronic stabilization, which should substantially reduce its free-ion dissociation constant. Hence, the inhibiting effects of lithium halides on the dehydrohalogenations mediated by lithium piperidide could also derive from common-ion rate depression.

On the Role of Solvation in Determining Reactivity. The results described herein raise a host of questions pertaining to solvation effects for which the answers are lacking. The most curious result is the dramatic seventh-order alkylation rate dependence on the THF concentration at the high concentration limit. With sterically hindered di- and tetramethyl THF derivatives as cosolvents, the seventh order can be crudely dissected into sterically dependent solvation and sterically independent medium effects. The rate increases observed when benzene is replaced by either Me_2THF or Me_4THF are attributed to long range, sterically independent medium effects. Within the experimental error of the rate measurements, a change of 5% of the bulk medium from benzene to a di- or tetrasubstituted THF—one molecule in 20—produces a detectable rate change. Although these effects are not large, their magnitude is still surprising if indeed they derive from changes in the bulk medium remote from the lithium center.

The approximate fifth-order rate dependence on the THF concentration observed in a medium of roughly constant dielectric strength appears to derive from sterically sensitive, short-range solvation effects. Although a variety of experimental and theoretical studies indicate that lithium ions will acquire a maximum of four monodentate ethereal ligands,[46] recent crystallographic studies of Power and co-workers provide evidence of a lithium ion bearing a weakly bound fifth THF ($Li^+(THF)_{4.5}$).[47] However, it seems highly unlikely that the lithium coordination sphere of monomeric or ion-paired Ph_2NLi could accept an additional four to six THF molecules. Although point charge based theoretical models afford solvation energies that are independent of the sign of the charge,[48] direct anion solvation is traditionally considered to be negligible in weakly polar, aprotic solvents.[48,49]

The explanation may come from recent calculations by Jorgensen and co-workers on the Na^+ ion in THF.[50] Along with an average primary coordination sphere of 5.7 THF molecules, they detected a secondary coordination sphere arising from THF dipole alignments with the methylene carbons of the coordinated THF's. Although the high primary sphere coordination numbers can be ascribed to the larger sodium ion radius, the four faces of a lithium-centered tetrahedron represent possible secondary coordination sites requiring occupation by oriented dipoles during ionization (Figure 9). In that the THF molecule in the secondary coordination shell would still be subjected to a sterically sensitive environment, only the unhindered parent THF molecules could effectively occupy these sites. In turn, if one is willing to broaden the definition of the activated complex to include the secondary solvation shell, then the high order in THF may accurately reflect the solvation stoichiometry.

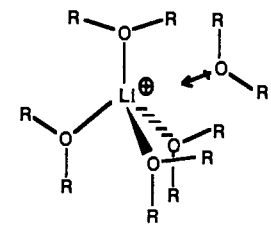

Figure 9.

Regardless of the explanation, it appears that the extraordinary solvent-dependent rates observed at the high THF concentration limits may eventually provide further insight into the solvation effects influencing organolithium reaction rates in more polar aprotic solvents such as DMSO and HMPA.[51,52]

Experimental Section

General Procedure. Benzene, tetrahydrofuran (THF), 2,5-dimethyltetrahydrofuran (Me_2THF), 2,2,5,5-tetramethyltetrahydrofuran (Me_4THF), hexane, pentane, diethyl ether, and cyclohexane were distilled from blue or purple solutions containing sodium benzophenone ketyl under vacuum. The hydrocarbon stills contained 1% tetraglyme to dissolve the ketyl. Hexamethylphosphoramide was distilled from sodium metal. *n*-Butyl bromide and *n*-octyl bromide were distilled from NaH or CaH_2 and stored with exclusion of light. Lithium diphenylamide and all other reagents and solvents were handled as described in the preceding paper.[14] Air- and moisture-sensitive materials were manipulated with standard glovebox and vacuum-line techniques with the aid of gas-tight syringes. Anhydrous, solvent-free $LiClO_4$ and $LiBPh_4$ were prepared via literature methods.[26,27]

Kinetics. A typical alkylation kinetic run was effected as follows. An oven-dried, 100-mL round-bottom flask equipped with gas adapters is charged with $Ph_2NLi_{solvent-free}$ (136 mg, 0.78 mmol), lithium bromide (67 mg, 0.78 mmol), and 20 mg of tetradecane (internal GC standard) in a glovebox. THF (1.89 mL, 23.3 mmol) is added to the flask followed by enough benzene (48 mL) to bring the volume to 50.0 mL. The flask is removed from the glovebox and heated to 51.2 ± 0.1 °C for at least 50 min. *n*-BuBr (2.5 mL, 23.4 mmol) is then added via syringe under argon purge. When larger quantities of *n*-BuBr are used, the *n*-BuBr is prewarmed to 51 °C to minimize temperature fluctuations. Aliquots of the reaction are periodically transferred by cannulation under positive argon flow into vials containing 1.0 mL of a 50:50 THF/95% ethanol mixture. The quenched aliquots are analyzed directly via capillary GC with correction for molar response. The course of the alkylations are monitored by the loss of the diphenylamine and formation of *n*-butyldiphenylamine relative to a tetradecane internal standard.

Runs using in situ generated Ph_2NLi were kinetically indistinguishable from those using premade Ph_2NLi. The procedure used was as follows. A 100-mL round-bottom flask equipped with gas inlet adapters is charged with LiBr (67 mg, 0.78 mmol), 3–4 mg of triphenylmethane indicator, and 20 mg of tetradecane GC standard. A 0.38 M solution of diphenylamine (2.0 mL, 0.76 mmol) in THF solution is added via syringe. The reaction flask is cooled to 0 °C and titrated with a 0.30 M ethyllithium/benzene solution until a faint pink color is noted. If the titration is in error by more than 7%, the run is terminated. Following addition of the remainder of the desired quantity of THF, enough benzene is added to bring the volume to 50.0 mL. The protocol is completed as described above.

Rate Constants and Statistics. All rate constants were calculated using first-order treatments and nonweighted linear least-squares fits. The reported errors correspond to one standard deviation. The observed rate constants were shown to be reproducible within ±3% by repetitions over

(46) (a) Solution studies; Popov, A. I. *Pure Appl. Chem.* **1975**, *41*, 275. (b) Gas phase studies; Castleman, A. W., Jr.; Holland, P. M.; Lindsay, D. M.; Peterson, K. I. *J. Am. Chem. Soc.* **1978**, *100*, 6039. (c) Theoretical studies, Kollman, P. A.; Kuntz, I. D. *J. Am. Chem. Soc.* **1974**, *96*, 4766. Jorgensen, W. L., unpublished studies on $+Li(THF)_4$. (d) Solid state studies; ref 40.

(47) Olmstead, M. M.; Power, P. P.; Sigel, G. *Inorg. Chem.* **1986**, *25*, 1027.

(48) Harned, H. S.; Owen, B. B. *The Physical Chemistry of Electrolytic Solutions*, 3rd ed.; Reinhold: New York, 1958.

(49) Burgess, J. *Metal Ions in Solution*; Wiley: New York, 1978.

(50) Jorgensen, W. L.; Chandrasekhar, J. *J. Chem. Phys.* **1982**, *77*, 5080.

(51) Bordwell, F. G.; Hughes, D. L. *J. Am. Chem. Soc.* **1986**, *108*, 7300.

(52) Within this paper we have not addressed the question of which, if any, of the reactive intermediates participate in single-electron transfer (SET) alkylations. We do note, however, that reaction of Ph_2NLi or $Ph_2NLi{\cdot}LiBr$ with 6-bromo-1-hexene under identical conditions used in the kinetic analyses provide $Ph_2N(CH_2)_4CH{=}CH_2$ to the exclusion (<1%) of the cyclized product throughout the entire THF concentration range.

a range of conditions. The first-order plots of the rate data measured in the high THF concentration limit (greater than 7.3 M) are reasonably linear to only 2.0 half-lives. Beyond 75% conversion, competitive elimination causes a distinct upward curvature whereas a measured fractional order causes downward curvature (see text). Various corrections of the raw kinetic data to account for the elimination pathway causes the calculated values of k_{obsd} to increase by up to 15%, and yet the calculated orders in *n*-butyl bromide and THF remain relatively unaffected. Hence, the reported pseudo-first-order rate constants were calculated from uncorrected raw data. The linear and nonlinear least-squares numerical fits were carried out with the LTPLOT statistical package developed within the Material Sciences Center at Cornell University.

Acknowledgment. We wish to thank the National Science Foundation Instrumentation Program (Grant CHE 7904825 and PCM 8018643) for support of the Cornell Nuclear Magnetic Resonance Facility and the A. P. Sloan Foundation for unrestricted support. We would also like to thank L. M. Jackman, A. Streitwieser, Jr., S. Webb, and R. Snaith for many helpful comments.

Registry No. BuBr, 109-65-9; Ph_2NLi, 5856-89-3; LiBr, 7550-35-8; *n*-octyl bromide, 111-83-1.

Exploratory Studies of the Transition Metal Catalyzed Intramolecular Cyclization of Unsaturated α,α-Dichloro Esters, Acids, and Nitriles[1]

Thomas K. Hayes, Rosanna Villani, and Steven M. Weinreb*

Contribution from the Department of Chemistry, The Pennsylvania State University, University Park, Pennsylvania 16802. *Received February 1, 1988*

Abstract: A general method for the synthesis of functionalized carbocyclic ring systems has been developed on the basis of the transition metal promoted intramolecular radical cyclizations of olefinic and acetylenic dichloro compounds (Kharasch-type reactions). Catalytic amounts of Ru or Fe complexes were shown to generate cyclopentanes **10**, **12**, **37**, and **38**, cyclohexanes **19** and **20**, bridged systems **25**, **26**, **31**, and **32**, and fused carbocycles **34** and **35** from a variety of readily available α,α-dichloro esters **4a–f**. Several α-chloro γ-lactones, **14**, **22–24**, **27**, **33**, and **36**, could be produced by the ruthenium or iron-catalyzed cyclization of α,α-dichloro acids **5a–e** or, alternatively, directly from the esters by using a dinuclear Mo catalyst. Most reactions showed a high degree of regioselectivity in the cyclization step. Equilibration of stereoisomers via a putative α-carboxylate radical intermediate (cf. **18**, **30**) was observed in some cases. Acetylenic α,α-dichloro esters **4g,h** afforded cyclopentanoid α,β-unsaturated esters **44** and **45** via the hydrogen atom abstraction/rearrangement mechanism proposed in Scheme X. Utilizing $CuCl/PPh_3$, intramolecular ring closure of a series of olefinic α,α-dichloro-β-keto esters **6** and α,α-dichloro nitriles **9** could be carried out to yield highly functionalized carbocycles **46–56**.

An impressive array of synthetically useful methodology has recently been developed for effecting intramolecular cyclizations of carbon-centered radicals with alkenes.[2] The large preponderance of these cyclizations has been of the 5-hexenyl radical type, and most cases have involved termination of the intermediate radical by hydrogen atom abstraction. One notable exception is the manganese(III) promoted cyclization of unsaturated β-keto esters and acids, extensively studied by Corey,[3] Fristad,[4] and Snider,[5] which terminates with carbon–oxygen bond formation and thus leaves the products in a more highly functionalized state.[6] A disadvantage of this particular method is that stoichiometric amounts of metal are required.

Over 4 decades ago, Kharasch et al.[7] made the important discovery that various halocarbons will add to olefins in a radical chain process to give adducts of type **1** (eq 1).[8] A more recent advance is the observation that this addition is catalyzed by a

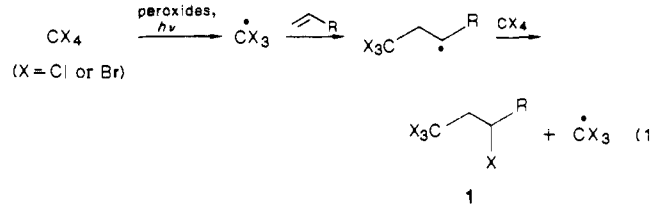

1

number of transition-metal complexes.[9,10] A primary advantage of these metal-promoted reactions is that teleomerization is minimized in most cases. This phenomenon is presumably due to the fact that metal-coordinated radicals are intermediates, the net result being that the rate of halide abstraction becomes faster than that of teleomerization.[11]

A known variation of the Kharasch reaction utilizes trichloroacetates and related α-chloro esters (Scheme I).[12] Interestingly, this addition can take two courses depending upon

(1) For a preliminary account of a portion of this work, see: Hayes, T. K.; Freyer, A. J.; Parvez, M.; Weinreb, S. M. *J. Org. Chem.* **1986**, *51*, 5501.
(2) For excellent reviews, see: Giese, B. *Radicals in Organic Synthesis: Formation of Carbon-Carbon Bonds*; Pergamon: New York, 1986. Ramaiah, M. *Tetrahedron* **1987**, *43*, 3541.
(3) Corey, E. J.; Kang, M. *J. Am. Chem. Soc.* **1984**, *106*, 5384.
(4) Fristad, W. E.; Peterson, J. R.; Ernst, A. B.; Urbi, G. B. *Tetrahedron* **1986**, *42*, 2489 and references cited therein.
(5) Snider, B. B.; Dombroski, M. A. *J. Org. Chem.* **1987**, *52*, 5489 and references cited therein.
(6) For other exceptions, see: (a) Curran, D. P.; Chen, M.-H.; Kim, D. *J. Am. Chem. Soc.* **1986**, *108*, 2489. (b) Kraus, G. A.; Landgrebe, K. *Tetrahedron* **1985**, *41*, 4039. (c) Patel, V. F.; Pattenden, G.; Russell, J. J. *Tetrahedron Lett.* **1986**, *27*, 2303. (d) Curran, D. P.; Kim, D. *Ibid.* **1986**, *27*, 5821. (e) Curran, D. P.; Chang, C.-T. *Ibid.* **1987**, *28*, 2477.
(7) Kharasch, M. S.; Jensen, E. V.; Urry, W. H. *Science (Washington, D.C.)* **1945**, *102*, 128.
(8) For a review, see: Walling, C.; Huyser, E. S. *Org. React. (N.Y.)* **1963**, *13*, 91.
(9) Kochi, J. K. *Organometallic Mechanisms and Catalysis*; Academic: New York, 1978. Minisci, F.; Citterio, A. *Adv. Free-Radical Chem.* **1980**, *6*, 65.
(10) For additional lead references, see: (a) Elzinga, J.; Hogeveen, H. *J. Org. Chem.* **1980**, *45*, 3957. (b) Bellus, D. *Pure Appl. Chem.* **1985**, *57*, 1827. (c) Grigg, R.; Devlin, J.; Ramasubbu, A.; Scott, R. M.; Stevenson, P. *J. Chem. Soc., Perkin Trans. 1* **1987**, 1515. (d) Martin, P.; Steiner, E.; Streith, J.; Winkler, T.; Bellus, D. *Tetrahedron* **1985**, *41*, 4057. (e) Tsuji, J.; Sato, K.; Nagashima, H. *Tetrahedron* **1985**, *41*, 5003. (f) Freidlina, R. K.; Velichko, F. K. *Synthesis* **1977**, 145.
(11) Recent mechanistic studies: Davis, R.; Groves, I. F. *J. Chem. Soc., Dalton Trans.* **1982**, 2281. Bland, W. J.; Davis, R.; Durrant, J. L. A. *J. Organomet. Chem.* **1984**, *260*, C75. Bland, W. J.; Davis, R.; Durrant, J. L. A. *Ibid.* **1984**, *267*, C45.
(12) (a) Murai, S.; Sonoda, N.; Tsutsumi, S. *J. Org. Chem.* **1964**, *29*, 2104. (b) Mori, Y.; Tsuji, J. *Tetrahedron* **1972**, *28*, 29. (c) Matsumoto, H.; Nikaido, T.; Nagai, Y. *J. Org. Chem.* **1976**, *41*, 396.

0002-7863/88/1510-5533$01.50/0